

Research Article

Segmentation of Killer Whale Vocalizations Using the Hilbert-Huang Transform

Olivier Adam

Laboratoire d'Images, Signaux et Systemes Intelligents (LiSSI - iSnS), Université de Paris 12, 61 avenue de Gaulle, 94010 Creteil Cedex, France

Correspondence should be addressed to Olivier Adam, adam@univ-paris12.fr

Received 1 September 2007; Revised 3 March 2008; Accepted 14 April 2008

Recommended by Daniel Bentil

The study of cetacean vocalizations is usually based on spectrogram analysis. The feature extraction is obtained from 2D methods like the *edge detection* algorithm. Difficulties appear when signal-to-noise ratios are weak or when more than one vocalization is simultaneously emitted. This is the case for acoustic observations in a natural environment and especially for the killer whales which swim in groups. To resolve this problem, we propose the use of the Hilbert-Huang transform. First, we illustrate how few modes (5) are satisfactory for the analysis of these calls. Then, we detail our approach which consists of combining the modes for extracting the time-varying frequencies of the vocalizations. This combination takes advantage of one of the empirical mode decomposition properties which is that the successive IMFs represent the original data broken down into frequency components from highest to lowest frequency. To evaluate the performance, our method is first applied on the simulated chirp signals. This approach allows us to link one chirp to one mode. Then we apply it on real signals emitted by killer whales. The results confirm that this method is a favorable alternative for the automatic extraction of killer whale vocalizations.

Copyright © 2008 Olivier Adam. This is an open access article distributed under the Creative Commons Attribution License, which permits unrestricted use, distribution, and reproduction in any medium, provided the original work is properly cited.

1. INTRODUCTION

Marine mammals show a vast diversity of vocalizations from one species to another and from one individual to another within a species. This can be problematic in analyzing vocalizations. The Fourier spectrogram remains today the classical time-frequency tool used by cetologists [1–3]—and sometimes the only one proposed—for use with typical software dedicated to bioacoustic sound analysis, such as MobySoft Ishmael, RainbowClick, Raven, Avisoft, and XBat, respectively, developed by [4–8].

In general, when analyzing bioacoustic sounds, posttreatment consists of binarizing the spectrogram by comparing the frequency energy to a manually fixed threshold [4, 9]. Then, feature extraction of the detected vocalizations is carried out using 2D methods specific to image processing. These algorithms, like the *edge detection* algorithm, are applied on the time-frequency representations [4, 5, 10].

Though the Fourier transform provides satisfactory results as far as cetologists are concerned, all hypotheses are not consistently verified. This is particularly true for the

analysis of continuous recordings when signals and noises are varying in time and frequency [11]. Moreover, these time-frequency representations have interference structures, especially for the type 1 Cohen's class (e.g., as the Wigner-Ville distribution) [12]. In addition, the uniform time-frequency resolution of the spectrogram has drawbacks for nonstationary signal analysis [13].

To overcome these difficulties, the following approaches have been recently proposed: parametric linear models such as autoregressive filters, Schur algorithm, and wavelet transform [14–17]. A comparative study of these approaches can be found in [16]. All of these methods are based on specific functions for providing the decomposition of the original signals. These functions can present a bias in the results proving a disadvantage in analyzing a large set of different signals, such as killer whale vocalizations. Also, concerning the wavelet transform, it should be noted that, in general, bioacoustic signals are never decomposed using the same wavelet family. For example, in analyzing the sperm whale regular clicks, authors have presented the Mexican hat wavelet, the wavelet package, and the Daubechies wavelet,

and so forth [15, 16, 18–20]. It seems that the choice to use one specific wavelet family is influenced less by the shape of the sperm whale click than by the global performance on the complete dataset used by the authors in their application.

Introduced as the generalization of the wavelet transform [21], the chirplet transform appears a possible solution in our application because of the specific shape of certain killer whale vocalizations (e.g., chirps). However, this method has some disadvantages. First, it requires the presegmentation of the signals (unnecessary in our method). Second, it is known that the computation time of the chirplet transform is lengthy and the proposed method to compensate for this drawback limits the analysis to one single chirp per presegment [21, 22]. This is not feasible for our approach because more than one vocalization is likely to be simultaneously present in the recordings.

This paper endeavors to adapt the Hilbert-Huang transform (HHT) to the killer whale vocalization detection and analysis. We introduce the HHT because it is well suited for nonlinear nonstationary signals analysis [12]. This transform is used as a reliable alternative to the wavelet transform for many applications [23, 24], including underwater acoustic sounds [25, 26]. The detailed advantages are promising for detecting underwater biological signals even if they have a wide diversity, as mentioned above. In our previous work, we have confirmed positive results for the analysis of sperm whale clicks using the HHT [27, 28].

In these articles, we demonstrated how to detect these transient signals emitted by sperm whales. The modes obtained from the HHT were used for extracting and characterizing sperm whale clicks, as detailed in [29]. We compared results from different approaches to obtain the best time resolution. First, this allowed us to characterize the shape of the emitted sounds (evaluation of the size of the sperm whale head with precision). Second, we optimized the computation of time delays for arrivals of the same sound on different hydrophones to minimize the error margin on the sperm whale localization. In conclusion, the HHT was presented as the alternative to the spectrograms.

Also, in these articles, we did not discuss the role of each mode obtained from the HHT and we did not present the method based on the combined modes as we do in this article. Considering that our current work is not only aimed at illustrating a new application of the HHT but also, through our application dedicated to killer whale vocalizations, we introduce an original method based on the combined modes detailed in the following section.

2. METHOD

Proposed by Huang et al. in 1998 [12], the Hilbert-Huang transform is based on the following two consecutive steps: (1) the empirical mode decomposition (EMD) extracts modes from the original signal. These modes are also referred to as intrinsic mode functions (IMFs), and (2) by applying the Hilbert transform on each mode, it is possible to provide time-frequency representation of the original signal. It is important to note that (1) the EMD is not defined by mathematical formalism; the algorithm can be found in [12],

and (2) the second step is optional. Some authors limit their application solely to the use of the EMD [30, 31].

The use of these modes can be compared to a filter bank [32]. At time k , the decreasing frequencies are placed in successive modes, from first to last. Our method takes advantage of this characteristic. Our contribution is an original process for the segmentation/combination of these modes. The objective is to link a single killer whale vocalization to a single mode.

2.1. Brief theory of the HHT

The EMD is applied on the original signal. This decomposition is one of the advantages of this method because no a priori functions are required: no function has to be chosen, and consequently, no bias results from this.

The EMD is based on the extraction of the upper and lower envelopes of the original signal (by extrema interpolation). The mode is extracted when (1) the number of the extrema and the number of zero crossings are equal to or differ at most by one, and (2) the mean of these two envelopes is equal to zero.

The original sampled signal $s(t)$ is

$$s(t) = \sum_{i=1}^M c_i(t) + R_M(t), \quad (1)$$

with $t, i, M \in N$. $t = 1, 2, \dots, T$, where T is the length of the signal s . M is the number of modes extracted from the signal using EMD. c_i is the i th IMF and R_M the residue. c_i and R_M are 1-dimension signals with T samples.

We note that the EMD could be applied on any nonzero-mean signal. However, each mode is a zero-mean signal. It is important to note that all the modes are monocomponent time-variant signals. The algorithm is shown in Figure 1.

The time-frequency representation is provided after computation of the Hilbert transform on each mode,

$$c_{\text{Hi}}(t) = \text{HT}(c_i) = c_i(t) \otimes \frac{1}{\pi t}, \quad (2)$$

where \otimes is the convolution.

From the analytic mode $c_{A_i}(t) = c_i(t) + jc_{\text{Hi}}(t)$, also written $c_{A_i}(t) = a_i(t)e^{j\theta_i(t)}$, we define the instantaneous amplitude response and the instantaneous phase. For each mode, the instantaneous frequency is obtained by

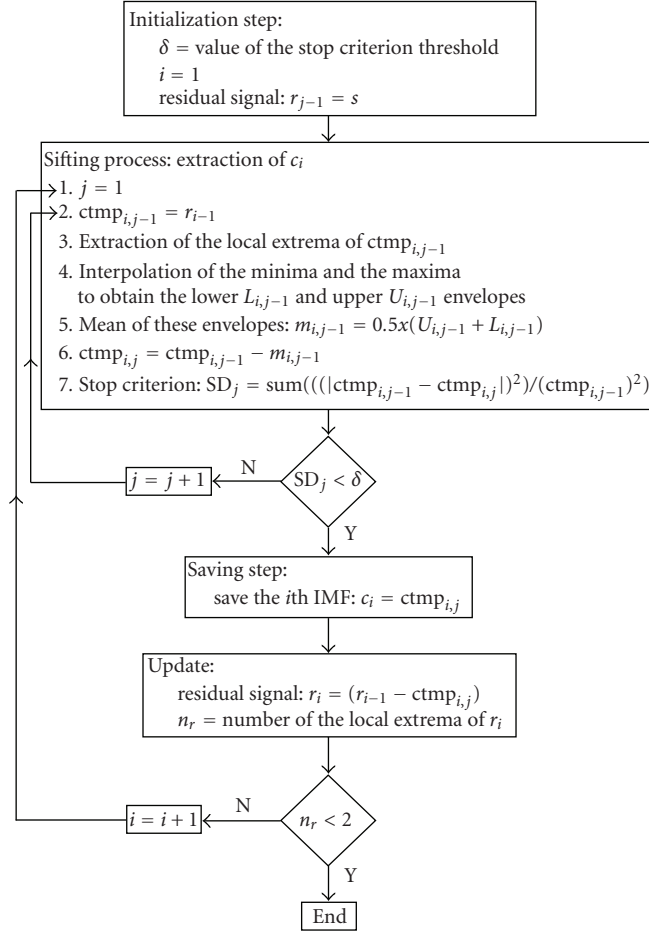
$$f_{c_i}(t) = \frac{1}{2\pi} \frac{d\theta_{c_i}(t)}{dt}. \quad (3)$$

Lastly, the time variations of the instantaneous frequencies of each mode correspond to the time-frequency representation.

2.2. Segmentation and combination of the modes

For cetologists, the acoustic observations of a specific marine zone consist of detecting sounds emitted by marine mammals. Once achieved, a feature extraction is carried out to identify the species.

It is possible to use the HHT in performing the emitted sound detection. We assume that the original zero-mean

FIGURE 1: Algorithm for the IMF extraction from the original signal s .

real signal has not been previously segmented by means of another technique. The EMD provides a limited number of modes (IMFs) resulting from this original signal. Note that each mode is the same length as the original signal (same number of samples). In any application, the challenge in using the HHT is in interpreting the contents of each mode as all signal components are divided between all the IMFs according to their instantaneous frequency [12]. For this reason, we propose the segmentation of the modes in order to link a part of this information to one single mode. Our method allows for segmentation to be based on the strong variations of the mode frequencies: these variations can be used to distinguish the presence of different chirps (cf. the example detailed in Section 3.1) or different vocalizations (cf. Section 3.2). Our segmentation is based on the three following rules: (1) all the modes are composed by the same number of segments, (2) the j th segments of all the modes have the same length, and (3) different segments of one single mode could be different lengths. To perform this segmentation, we could have used a criterion based on the discontinuities of the instantaneous amplitude. But vocalizations show a continuous fundamental frequency (signal with a constant or time-varying frequency) in their complete duration (time between two silences like that which

the human ear can hear). Also, for our purposes, we have chosen to work with variations of the frequencies because we want to track killer whale vocalizations. Moreover, tracking the frequency variations for extracting the killer whale vocalizations is possible because these frequencies are much higher in pitch than the underwater ambient noise.

The detection of the frequency variations helps us identify the exact beginning and end of each vocalization. For the detection approach, our criterion is based on the derivative of the instantaneous frequency. But it is important to keep in mind that the phase is a local parameter. To avoid fluctuations due mainly to ambient noise, Cexus et al. have recently proposed the use of the Teager-Kaiser operator [33]. But this seemingly promising operator has not been evaluated for our application. Up to now, we calculate the derivative of the mean instantaneous frequency for establishing the limits of all segments for one mode,

$$g_{c_i}(t) = \frac{d\bar{f}_{c_i}(t)}{dt}, \quad (4)$$

where \bar{f}_{c_i} is the mean of the successive instantaneous frequencies. This step is added for attenuating the variations

of these instantaneous frequencies. \bar{f}_{c_i} is the median of f_{c_i} :

$$\bar{f}_{c_i}(t) = \frac{1}{T_w} \sum_{k=-T_w/2}^{T_w/2} f_{c_i}(t-k). \quad (5)$$

The length T_w of the time window for providing this mean depends on the application. In this paper, the T_w value is empirically established from the study of our dataset.

The idea of our detection approach is to track the signal via analysis of the functions g_{c_i} . These functions correspond to the frequency variations of each monocomponent IMF. Strong variations in these IMFs which indicate the presence of signal information (start or end of one vocalization) provoke notable changes in the functions g_{c_i} , hypothesis H_0 . Otherwise, these functions are nearly constant, hypothesis H_1 . The functions d_{c_i} are given by

$$d_{c_i}(t) = (g_{c_i}(t) - g_{c_i}(t-1))^2 \underset{H_0}{\overset{H_1}{\geq}} \eta, \quad (6)$$

where η denotes the comparison threshold. For our application, this value is constant ($\eta = 10\% \times \max(d_{c_i})$), but it could be made adaptive.

When a new vocalization appears in the recordings, the function g_{c_i} calculated from the first mode is suddenly varying. The value of the detection criterion d_{c_i} is superior to the threshold η .

Moreover, this function g_{c_i} will have a positive maximum and a negative maximum, respectively, for the start and the end of one single vocalization as the vocalization frequencies are currently higher than the low ambient noise frequencies.

Moreover, because two vocalizations have two different main frequencies, g_{c_i} will present discontinuities, which are used for the vocalization segmentation.

Our criterion is successively applied on the first mode, then the second mode, and so on. At the end of this process, we obtain all the segments and we can determine their length.

The i th IMF is

$$c_i = \{c_i^1 | c_i^2 \cdots | c_i^N\}, \quad (7)$$

with c_i^j being the j th segment of c_i defined by

$$c_i^j = \{c_i(t_{j-1} + 1), c_i(t_{j-1} + 2), \dots, c_i(t_j + 1), c_i(t_j)\}, \quad (8)$$

where t_{j-1} and t_j are the time of the last sample of segments c_i^{j-1} and c_i^j , respectively. Note that $t_0 = 0$ and $t_N = T$.

In our approach, we validate either the decreasing shift or the permutation of the j th segments between two modes c_{i-1} and c_i . These combinations allow us to link specific information to one single IMF. Our objective is to track the fundamental frequency and the harmonics of the killer whale vocalizations (see Section 3). Each vocalization will be linked to one mode.

The new mode m is the result of the combined previous IMF,

$$m_i = \{c_k^1 | c_k^2 \cdots | c_k^j | \cdots | c_k^N\}. \quad (9)$$

The combination depends on the positive or negative maximum of g_{c_i} , when $d_{c_i}(t) > \eta$.

(i) $\max(g_{c_i}) > 0$. This means that the instantaneous frequency of the end of segment c_i^j is less than the instantaneous frequency of the start of the next segment c_i^{j+1} . Concerning segment c_i^j , the vocalization could continue on segment c_{i+1}^{j+1} . So, our process consists of switching this segment c_i^j to the new m_{i+1}^j and putting zeros z_i^j in the new m_i^j ,

$$z_i^j = \left\{ \underbrace{0}_{z_i(t_{j-1}+1)}, \underbrace{0}_{z_i(t_{j-1}+2)}, \dots, \underbrace{0}_{z_i(t_j-1)}, \underbrace{0}_{z_i(t_j)} \right\}. \quad (10)$$

We repeat this process on the segment of each following mode: $m_{k+1}^j = c_k^j$ with $k \geq i$. Whereas segment c_i^{j+1} is the start of a new vocalization. Our process does not modify this segment or those that follow.

(ii) $\max(g_{c_i}) < 0$. The instantaneous frequency of the end of segment c_i^j is higher than the instantaneous frequency of the start of the next segment c_i^{j+1} . This means that segment c_i^j marks the end of the vocalization. This segment is not modified. All the following segments c_k^l ($l \geq j+1$) of this mode are switched to the next mode ($k+1$): $m_{k+1}^l = c_k^l$ and we replace the current segments with zeros z_k^l .

This process is summarized in Table 1.

This process of combining is done from the first to the last IMF. Because the number of modes and the number of segments are finite, the process ends on its own.

The new obtained signal is 1-dimensional with T samples and is given by

$$u = \left\{ \sum_{i=1}^M m_i^1 \mid \sum_{i=1}^M m_i^2 \cdots \mid \sum_{i=1}^M m_i^N \right\}. \quad (11)$$

The following step is optional. We use a weighted factor ($\lambda_i^j \in \mathfrak{R}$) on each segment,

$$u = \left\{ \sum_{i=1}^M \lambda_i^1 m_i^1 \mid \sum_{i=1}^M \lambda_i^2 m_i^2 \cdots \mid \sum_{i=1}^M \lambda_i^N m_i^N \right\}. \quad (12)$$

We diminish the role of each segment by using low values of the weighted factors; we can even delete certain segments by using $\lambda_i^j = 0$. Consequently, this step allows us to amplify or attenuate one or more segments of the combined IMF. The value of these weighted coefficients must be chosen based on the objective of the application. In many cases, it could be appropriate to fix a value dependent on the signal frequencies. In our application, we amplify the highest frequencies and attenuate the lowest frequencies in relation to the killer whale vocalizations and the ambient noise, respectively—we use our process like a filter. In other applications, the objective could be to use a criterion based on the signal energy, for example, to reduce high-energy segments and amplify low-energy segments.

Equation (12) demonstrates the possibility of using the new IMF for the selection of certain parts of the original signal.

TABLE 1: Combination of segments; case 1: $\max(g_{c_i}) > 0$; case 2: $\max(g_{c_i}) < 0$ (the dotted line is the separation of 2 successive segments).

Cases	Actions ($k \geq i, l \geq j + 1$)		Remarks	
1.		Segments m_k^j $z_i^j \rightarrow m_i^j$ $c_i^j \rightarrow m_{i+1}^j$ $c_{i+1}^j \rightarrow m_{i+2}^j$ $c_{i+2}^j \rightarrow m_{i+3}^j$ \vdots	Segments m_k^l No change	segment c_{i+1}^j could be the continuation of segment c_i^{j+1} (possible parts of the same vocalization)
2.		Segments m_k^j No change	Segments m_k^l $z_i^l \rightarrow m_i^l$ $c_i^l \rightarrow m_{i+1}^l$ $c_{i+1}^l \rightarrow m_{i+2}^l$ $c_{i+2}^l \rightarrow m_{i+3}^l$ \vdots	Segment c_{i+1}^j is the last part of the vocalization All segments c_k^l are switched to the segments c_{k+1}^l

3. RESULTS

Our research team is involved in a scientific project based on the detection and localization of marine mammals using passive acoustics. We have already used the HHT for different kinds of bioacoustic transient signals, particularly sperm whale clicks [27]. Now, we are applying the method on harmonic signals. In this section, we show the results obtained on simulated chirps, then we illustrate its performance on killer whale vocalizations.

3.1. Analysis of the simulated three chirps signal

To present our method in detail, we have generated a simulated signal composed of the three chirps with varying frequencies (linear, convex, or concave) (Figure 2(A)).

The normalized frequencies of the first chirp s_1 vary from 0.062 to 0.022. s_2 is the second chirp having a concave variation of the normalized frequency from 0.016 to 0.08. s_3 is the third chirp containing the linear variation of the normalized frequency from 0.008 to 0.012.

In this example, we use normalized frequency as it is important to know the frequencies of the chirps rather than the value of the sampling frequency.

The spectrogram is provided in Figure 2(B).

The first step of our approach involves performing the EMD (Figure 2(C)). We note that the three first modes present all the frequency variations of the three chirps.

Providing the time-frequency representation of all these modes will reveal the frequencies of each chirp. With the EMD, these frequencies are hierarchically allocated to each mode, meaning that at each moment, the first mode has the highest frequency and the last mode, the lowest frequency.

Figure 2(D) shows that the IMFs have frequencies originating from all three chirps. Therefore, IMF 1 successively contains the frequencies from chirp s_3 , then from s_1 , then from s_2 , and then from s_3 again. Similarly, IMF 2 is composed of frequencies from s_3 , then s_2 , and s_3 again. Finally, IMF 3 contains only a short part of the frequency of s_3 .

Feature extraction from the time-frequency representation (Figure 2(B)) requires 2D algorithms, such as the *edge detection* algorithm, for example. Our goal allows us to avoid using these algorithms so common in image processing.

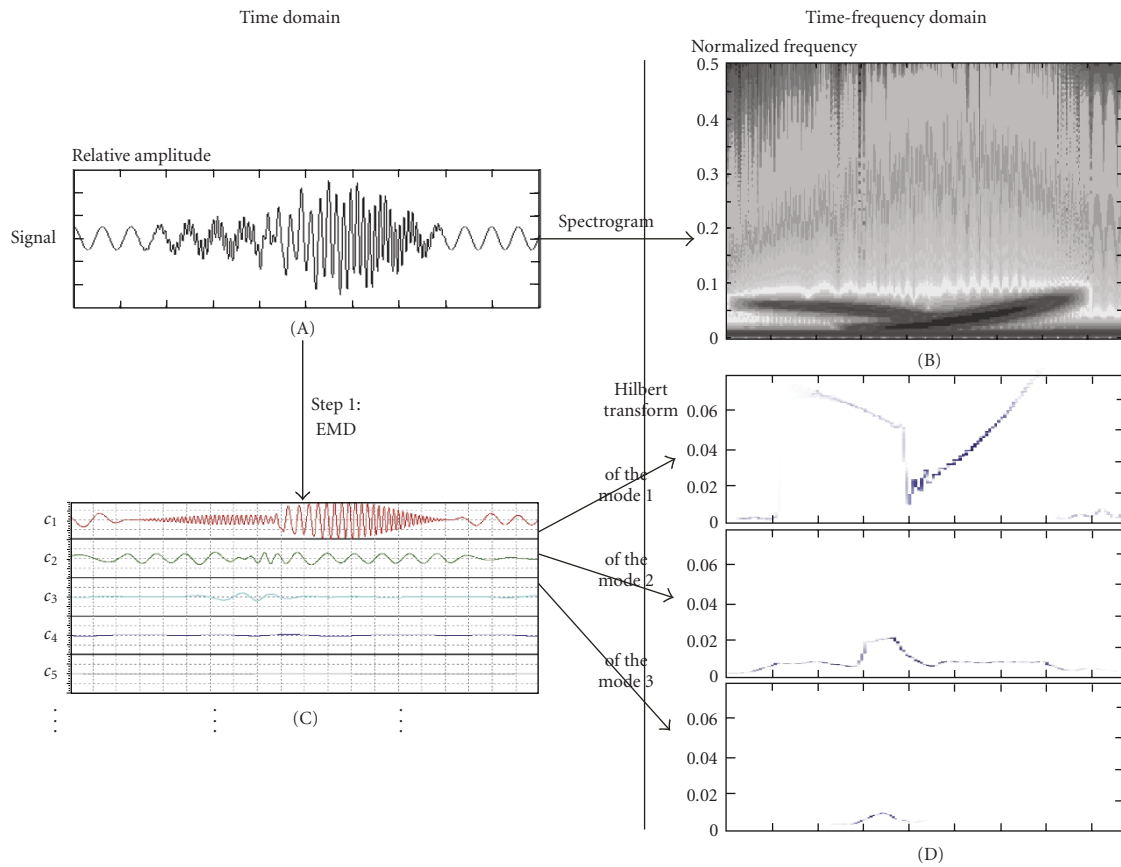
In our simulated signal analysis, the work results in linking one complete chirp to one single IMF. The point of using the new combined IMF is that the new IMF 1 receives its frequency solely from chirp s_1 . New IMF 2 and IMF 3 will, respectively, receive frequencies solely from s_2 and s_3 (6).

To segment these IMFs, we monitor the variations of the g_{c_i} parameter (Figure 2(E)). In our example, the five segments are obtained from this parameter (Figure 2(F)). Note that to avoid the side effects resulting from the segmentation process, we force the segments to start and end at zero by applying the Tukey window [34].

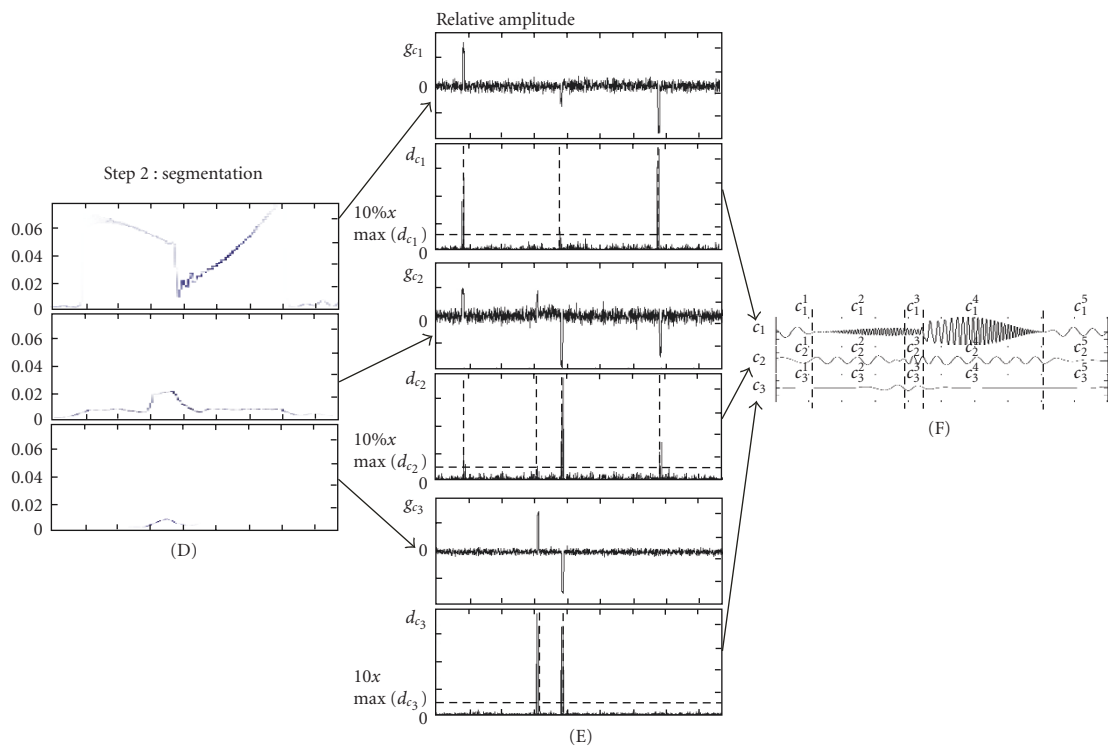
Then, the IMFs are combined (see (6) and Figure 2(G)). We provide the time-frequency representation. The Hilbert transform is applied on these new combined IMFs. Thus, the obtained figure confirms that the new IMFs have the frequencies of the original chirps.

If one of these chirps is considered a source of noise, we could discard this chirp by using the weighted coefficients equal to zero. For example, we can delete m_3 by applying $\lambda_3^j = 0$.

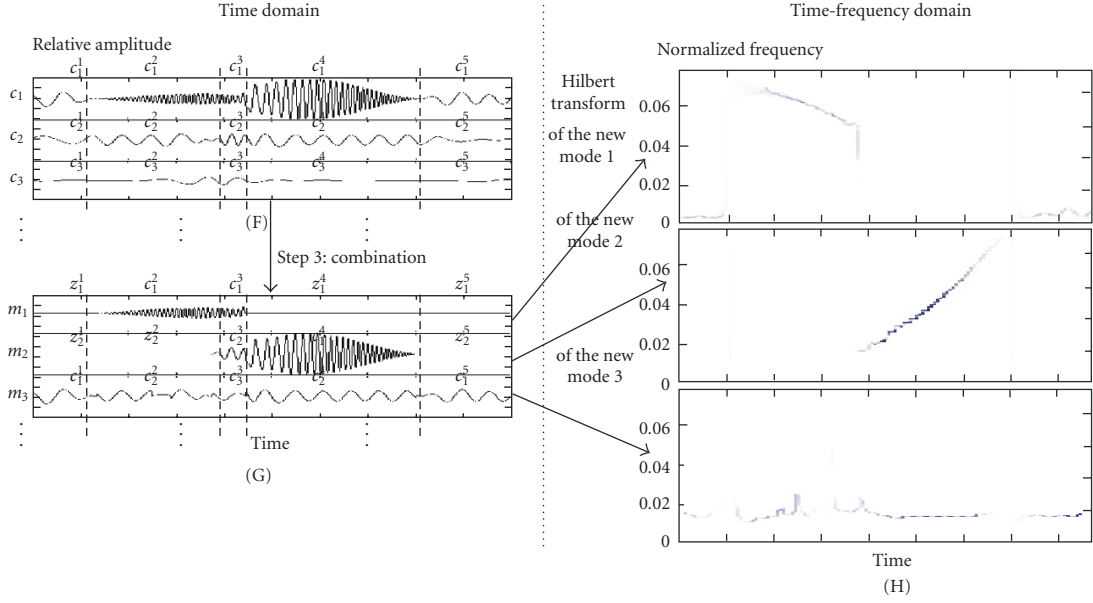
The advantage is that we can use a 1D algorithm to extract the frequency from each new IMF (in our case, the interpolation could be done by using a simple 1-order or



(a) Decomposition of the original simulated signal; (A) original signal with the three chirps, (B) spectrogram, (C) EMD decomposition, (D) Hilbert transform of each IMF



(b) Segmentation of the IMFs; (D) Hilbert transform of each IMF, (E) computation of g_{c_i} and d_{c_i} , (F) segmentation of the IMFs



(c) Combination of the IMFs; (F) segmentation of the IMFs, (G) new combined IMFs, (H) Hilbert transform applied on these new IMFs

FIGURE 2

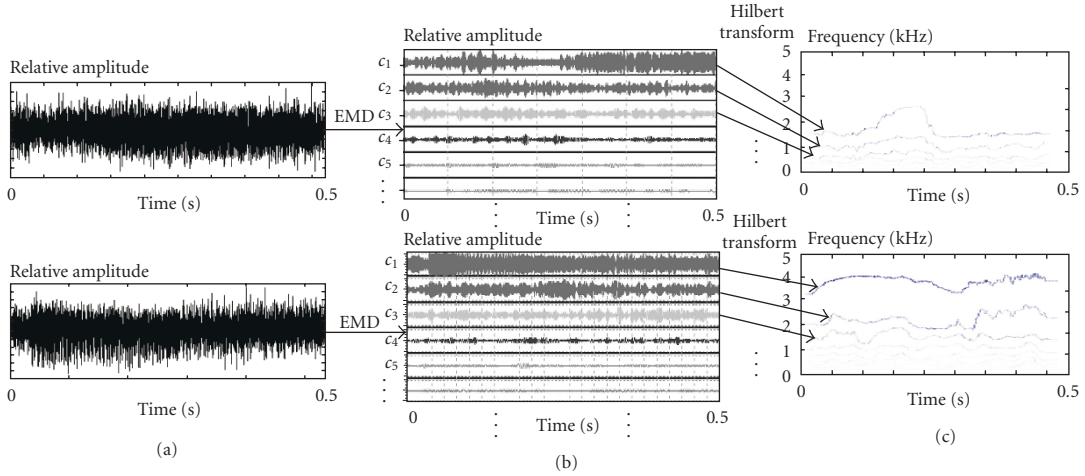


FIGURE 3: Decomposition of two harmonic killer whale vocalizations; (a) original signal, (b) EMD, (c) Hilbert transform of each new IMF.

2-order polynomial regression). We do not have to employ 2D algorithms.

In conclusion, we have linked one chirp to one single new IMF. We have shown too that it is possible to filter the signal through this method.

3.2. Analysis of killer whale vocalizations

Killer whales emit vocalizations with various time and frequency characteristics (short, long, with or without harmonics, etc.). Killer whales live and evolve in social groups, so it is very rare to have recordings from only one individual, unless we consider the animals in the aquarium. Therefore, in these recordings, it is current to find more than one vocalization

at the same time. This complicates the detection of these vocalizations. Another challenge is to find one complete vocalization. At times, a single complete vocalization is segmented into many components. This depends on the method used to provide the time-frequency representation. When the signal-to-noise ratio is weak, it is common that the binarized spectrogram separately extracts different parts of one single vocalization. To prevent this, other methods have been proposed like the chirplet transform and the wavelet transform [16, 21, 25].

In our dataset, the vocalizations have been recorded from a group of killer whales in their natural environment. Vocalization segmentation is commonly accomplished by applying the spectrogram. The analysis of this time-frequency

TABLE 2: Detection of vocalizations; % of detection of complete vocalizations, % of detection of simultaneous vocalizations.

Detection of vocalizations	Spectrogram	Chirplet transform	Combined IMFs
Complete	76.9	95	95
Simultaneous	78	31.7	92.7

representation is executed with the aid of a threshold to binarize the spectrogram, or of an edge detector [4, 5]. The performance depends on (1) the signal-to-noise ratio which is varying during all the recordings, and (2) the simultaneous presence of more than one vocalization. Our method was introduced as a solution to overcome these two obstacles. First, the ambient noise has lower frequencies than the vocalizations. So it is coded by the last IMFs. Second, each vocalization is linked to a single combined IMF. This facilitates feature extraction (duration of the vocalization, start and end frequencies, and shape).

In our application, we do not take into account the last IMFs. In our previous work [27], we defined a performance/complexity criterion based on the contribution of each mode for obtaining the complete original signal. Applied on this dataset, this criterion shows that only the first five IMFs are sufficient for extracting killer whale vocalizations. This low number of IMFs is coherent with the results obtained by Wang et al. [25]. Considering only the first five IMFs contributes to minimize the execution time of this approach.

In the second step of the process, the modes are combined following our algorithm to link one vocalization to one mode.

We have compared the detection performance of the three methods: the spectrogram, the chirplet transform, and our approach based on the combined IMFs. Results appear in Table 2. We consider our detection to be accurate when the vocalization is determined in its full length. The segmented vocalization is considered to be falsely detected.

When using the spectrogram, detection quality depends mainly on the threshold value. In this application, we have used a fixed threshold for the complete dataset in spite of the presence of the varying ambient noise. The consequence is that 25% of the vocalizations are segmented. Thus, the spectrogram detector extracts many successive vocalizations that are in fact all components of the same vocalization. These results could be slightly improved by using an adaptive threshold.

With the chirplet transform, the results decrease significantly in the presence of simultaneous vocalizations. In these cases, it seems that the algorithm extracts the vocalization containing the greatest energy. Our method is more robust because these different vocalizations are linked to different combined modes. The detection process is done on each mode.

Another advantage of our approach concerns vocalizations with harmonics. The presence of these harmonics helps biologists characterize and classify sounds emitted by animals. Our method equally enables linking one harmonic

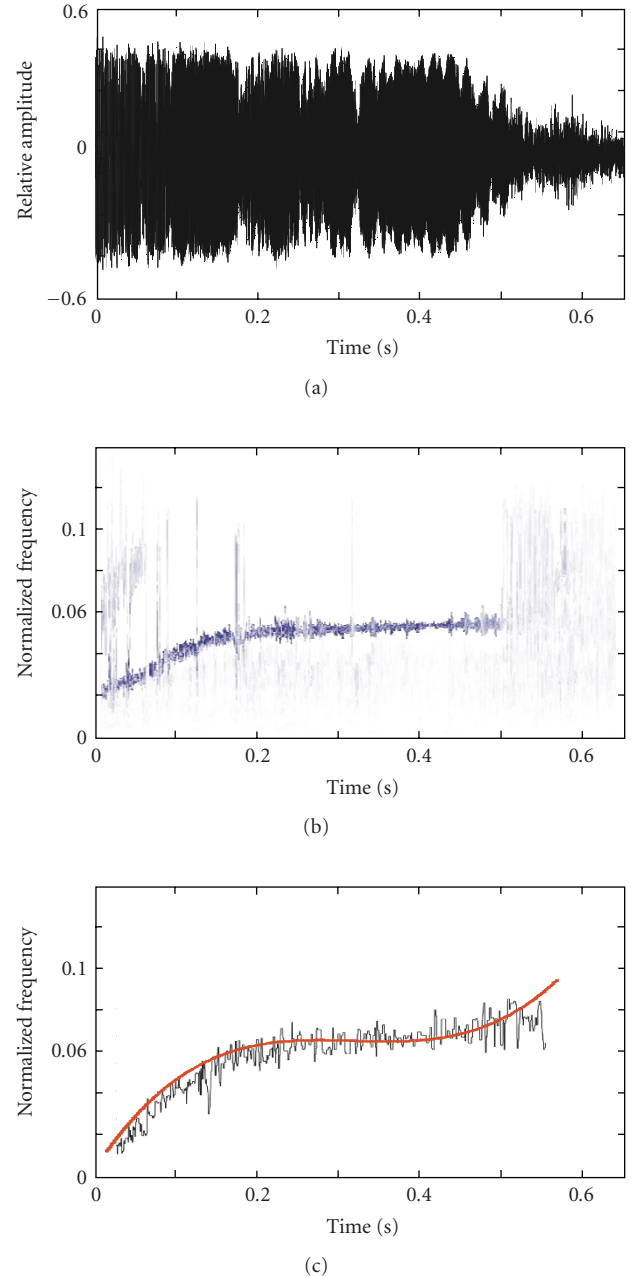


FIGURE 4: Extraction of the vocalization features; (a) original signal, (b) Hilbert transform, (c) characterization of the vocalization.

to a single mode (as seen in Figure 3). Unlike in the previous case, the vocalizations with harmonics are distinguishable from simultaneous vocalizations because all the harmonic components have the same shape.

Another advantage of our method is that it allows us to easily characterize each vocalization by applying the Hilbert transform on each combined mode m_i (duration, start and end frequency, and shape). We employ a simple 1D function to model the vocalizations. This is illustrated on a sample of our dataset (Figure 4); we have extracted the start and the end of the vocalization and the shape by applying a 3-order polynomial regression.

4. CONCLUSION

After achieving promising results obtained on sperm whale clicks (transient signals), our objective is to evaluate the Hilbert-Huang transform on harmonic killer whale vocalizations. To this end, we propose a new method based on an original combination of the intrinsic mode functions obtained by the empirical mode decomposition. The advantages of our method are (1) we filter the signal from the new combined modes; (2) we link one vocalization (or one harmonic) to one single mode; (3) we use a 1D algorithm to characterize the vocalizations.

ACKNOWLEDGMENT

This work was supported by Association DIRAC (France).

REFERENCES

- [1] J. Cirillo, S. Renner, and D. Todt, "Significance of context-related changes in compositions and performances of group-repertoires: evidence from the vocal accomplishments of orcinus orca," in *Proceedings of the 20th Annual Conference of the European Cetacean Society*, pp. 70–71, Gdynia, Poland, April 2006.
- [2] A. Kumar, "Animal communication," *Current Science*, vol. 85, no. 10, pp. 1398–1400, 2003.
- [3] W. A. Kuperman, G. L. D'Spain, and K. D. Heaney, "Long range source localization from signal hydrophone spectrograms," *Journal of the Acoustical Society of America*, vol. 109, no. 5, pp. 1935–1943, 2001.
- [4] D. Mellinger, "Automatic detection of regularly repeating vocalizations," *Journal of the Acoustical Society of America*, vol. 118, no. 3, p. 1940, 2005.
- [5] D. Gillespie, "Detection and classification of right whale class using an edge detector operating on smoothed spectrogram," *Journal of the Canadian Acoustical Association*, vol. 32, pp. 39–47, 2004.
- [6] R. A. Charif, D. W. Ponirakis, and T. P. Krein, "Raven Lite 1.0 User's Guide," Cornell Laboratory of Ornithology, Ithaca, NY, USA, 2006.
- [7] R. Specht, www.avisoft.de.
- [8] H. Figueroa, "Acoustic tool development with XBAT," in *Proceedings of the 2nd International Workshop on Detection and Localization of Marine Mammals Using Passive Acoustics*, p. 53, Monaco, France, November 2005.
- [9] S. Jarvis, D. Moretti, R. Morrissey, and N. Dimarzio, "Passive monitoring and localization of marine mammals in open ocean environments using widely spaced bottom mounted hydrophones," *Journal of the Acoustical Society of America*, vol. 114, no. 4, pp. 2405–2406, 2003.
- [10] C. Hory, N. Martin, and A. Chehikian, "Spectrogram segmentation by means of statistical features for non-stationary signal interpretation," *IEEE Transactions on Signal Processing*, vol. 50, no. 12, pp. 2915–2925, 2002.
- [11] C. Ioana and A. Quinquis, "On the use of time-frequency warping operators for analysis of marine-mammal signals," in *Proceedings of IEEE International Conference on Acoustics, Speech and Signal Processing (ICASSP '04)*, vol. 2, pp. 605–608, Montreal, Canada, May 2004.
- [12] N. E. Huang, Z. Shen, S. R. Long, et al., "The empirical mode decomposition and the Hilbert transform spectrum for nonlinear and non-stationary time series analysis," *Proceedings of the Royal Society A*, vol. 454, no. 1971, pp. 903–995, 1998.
- [13] R. Tolimieri and M. An, *Time-Frequency Representations, Applied and Numerical Harmonic Analysis*, Birkhäuser, Boston, Mass, USA, 1997.
- [14] S.-H. Chang and E.-T. Wang, "Application of the robust discrete wavelet transform to signal detection in underwater sound," *International Journal of Electronics*, vol. 90, no. 6, pp. 361–371, 2003.
- [15] R. Huele and H. Udo de Haes, "Identification of individual sperm whales by wavelet transform of the trailing edge of the flukes," *Marine Mammal Science*, vol. 14, no. 1, pp. 143–145, 1998.
- [16] M. Lopatka, O. Adam, C. Laplanche, J. Zarzycki, and J.-F. Motsch, "An attractive alternative for sperm whale click detection using the wavelet transform in comparison to the Fourier spectrogram," *Aquatic Mammals*, vol. 31, no. 4, pp. 463–467, 2005.
- [17] M. Lopatka, O. Adam, C. Laplanche, J. Zarzycki, and J.-F. Motsch, "Effective analysis of non-stationary short-time signals based on the adaptive schur filter," *Transactions on Systems, Signals & Devices*, vol. 1, no. 3, pp. 295–319, 2005.
- [18] M. P. Fargues and R. Bennett, "Comparing wavelet transforms and AR modelling as feature extraction tools for underwater signal classification," in *Proceedings of the 29th Asilomar Conference on Signals, Systems and Computers*, vol. 2, pp. 915–919, Pacific Grove, Calif, USA, October–November 1995.
- [19] J. Ioup and G. Ioup, "Identifying individual sperm whales acoustically using self-organizing maps," *Journal of the Acoustical Society of America*, vol. 118, no. 3, p. 2001, 2005.
- [20] M. van der Schaar, E. Delory, A. Català, and M. André, "Neural network-based sperm whale click classification," *Journal of the Marine Biological Association of the UK*, vol. 87, no. 1, pp. 35–38, 2007.
- [21] S. Mann and S. Haykin, "The chirplet transform: physical considerations," *IEEE Transactions on Signal Processing*, vol. 43, no. 11, pp. 2745–2761, 1995.
- [22] J. Cui, W. Wong, and S. Mann, "Time-frequency analysis of visual evoked potentials using chirplet transform," *Electronics Letters*, vol. 41, no. 4, pp. 217–218, 2005.
- [23] N. E. Huang, C. C. Chern, K. Huang, L. W. Salvino, S. R. Long, and K. L. Fan, "A new spectral representation of earthquake data: Hilbert spectral analysis of station TCU129, Chi-Chi, Taiwan, 21 September 1999," *Bulletin of the Seismological Society of America*, vol. 91, no. 5, pp. 1310–1338, 2001.
- [24] P. Hwang, J. Kaihatu, and D. Wang, "A comparison of the energy flux computation of shoaling waves using Hilbert and wavelet spectral analysis technique," in *Proceedings of the 7th International Workshop on Wave Hindcasting and Forecasting*, Banff, Canada, October 2002.
- [25] F.-T. Wang, S.-H. Chang, and J. C.-Y. Lee, "Signal detection in underwater sound using the empirical mode decomposition," *IEICE Transactions on Fundamentals of Electronics, Communications and Computer Sciences*, vol. E89-A, no. 9, pp. 2415–2421, 2006.
- [26] A. D. Veltcheva and C. G. Soares, "Identification of the components of wave spectra by the Hilbert-Huang transform method," *Applied Ocean Research*, vol. 26, no. 1-2, pp. 1–12, 2004.
- [27] O. Adam, "The use of the Hilbert-Huang transform to analyze transient signals emitted by sperm whales," *Applied Acoustics*, vol. 67, no. 11-12, pp. 1134–1143, 2006.
- [28] O. Adam, "Advantages of the Hilbert-Huang transform for marine mammals signals analysis," *Journal of the Acoustical Society of America*, vol. 120, no. 5, pp. 2965–2973, 2006.

- [29] M. A. Chappell and S. J. Payne, "A method for the automated detection of venous gas bubbles in humans using empirical mode decomposition," *Annals of Biomedical Engineering*, vol. 33, no. 10, pp. 1411–1421, 2005.
- [30] P. J. Oonincx and J.-P. Hermand, "Empirical mode decomposition of ocean acoustic data with constraint on the frequency range," in *Proceedings of the 7th European Conference on Underwater Acoustics*, Delft, The Netherlands, July 2004.
- [31] I. M. Jánosi and R. Müller, "Empirical mode decomposition and correlation properties of long daily ozone records," *Physical Review E*, vol. 71, no. 5, Article ID 056126, 5 pages, 2005.
- [32] P. Flandrin, G. Rilling, and P. Gonçalves, "Empirical mode decomposition as a filter bank," *IEEE Signal Processing Letters*, vol. 11, no. 2, pp. 112–114, 2004.
- [33] J. C. Cexus, A. O. Boudraa, L. Guillon, and A. Khenchaf, "Sonar targets analysis by Huang Teager Transform (THT)," Colloque Sea Tech Week, CMM 2006.
- [34] R. B. Blackman and J. W. Tukey, *The Measurement of Power Spectra from the Point of View of Communication Engineering*, Dover, Mineola, NY, USA, 1958.